Journal of the Korean Society of Surveying, Geodesy, Photogrammetry and Cartography
Vol. 34, No. 6, 591-596, 2016
https://doi.org/10.7848/ksgpc.2016.34.6.591
ISSN 1598-4850(Print)
ISSN 2288-260X(Online)
Original article

Investigation of Crustal Deformation due to the Kyungju Earthquake in 2016

Hong, Chang-Ki[1)]

Abstract

The M_w=5.8 Kyungju (South Korea) earthquake took place on 12 September 2016. This event may cause deformation around Kyungju city, located in the southeastern part of the Korean peninsula. In this study, GPS data was collected from the 17 Korean CORS and processed to determine the deformation. Minimum constraint solutions, to avoid the network distortion, are obtained and an S-transformation is applied to the coordinate difference vector and its covariance matrix for comparisons. In the final step, a statistical test is performed to determine the deformation due to the Kyungju earthquake. Based on the results, it was found that there is no significant deformation around Kyungju city. Hence, it can be said that the re-measurement or re-establishment of the geodetic control points in South Korea is not required.

Keywords : GPS, Deformation, Kyungju Earthquake, S-transformation

1. Introduction

The GPS (Global Positioning System) can provide precise positions in 3 dimensional space and, as a consequence, it has been widely used for crustal deformation analysis (Hager *et al*., 1991; Erdoğan *et al*., 2009; Liu *et al*., 2014). GPS is also known to be an efficient tool to monitor deformation because it is not affected by weather conditions and continuous data collection is available. The coordinates of specific points may be estimated in absolute or in relative positioning mode using the GPS. It is notable that absolute positioning does not provide enough positioning accuracy, unlike relative positioning. However, the relative positioning technique has an inherent drawback, i.e., the datum defect of the system of observations (Papo and Stelzer, 1985; Ananga, 1991; Even-Tzur, 2011). To overcome this drawback, solutions can be obtained by fixing one of station coordinates, or applying stochastic constraints on some station coordinates. This may lead to network distortion, which is not suitable for deformation analysis, hence the minimum constraint (also called free net or trace-minimum) approach is usually adopted for deformation analysis. For the minimum constraint solution, the network geometry is retained. Nevertheless, two solutions cannot be directly compared as each solution may refer to different datum. Hence, the transformation from one datum to another, without performing an additional adjustment, should be applied using the so-called S-transform (Barda, 1973; Denli, 2004). Time series analysis can also be used to detect the deformation by analyzing the coordinate variations with respect to time (Miura *et al*., 2002; Hamdy *et al*., 2005; Lin *et al*., 2010). In this case, ITRF (the International Terrestrial Reference Frame) stations located outside of the network may

Received 2016. 11. 24, Revised 2016. 11. 30, Accepted 2016. 12. 21
1) Member, Dept. of Geoinformatics Engineering, Kyungil University (E-mail: ckhong@kiu.ac.kr)

be required so that the estimated coordinates are consistent with ITRF. However, the estimated coordinates are dependent on the selected datum, which may degrade the capability of detecting the subtle deformation.

In this study, the assessment of deformation due to the Kyungju earthquake occurred on 12 September 2016. Kyungju city is located in the southeastern parts of the Korean peninsula and deformation around the city may have occurred, considering the 5.8 magnitude earthquake. To investigate the possible deformation, the GPS data collected from the CORS (Korean Continuously Operating Reference Station) is processed and analyzed. The determination of the deformation is then performed through the statistical test.

2. Methodology

The computation of the positions of the points with reliable accuracy in two periods is required for the deformation analysis. For this purpose, the positioning can be performed using the GPS measurements through the least-squares adjustment method. The double differenced observations in the relative positioning mode are usually used to eliminate or reduce the inherent errors, so that precise positioning results can be obtained. The linearized observation equation for the GPS measurements in the Gauss-Markov adjustment model is as follows (Snow, 2002; Schaffrin, 2003):

$$\mathbf{y} = \mathbf{A}\boldsymbol{\xi} + \mathbf{e}, \quad \mathbf{e} \sim \left(0, \sigma_0^2 \mathbf{P}^{-1}\right), \quad rk(\mathbf{A}) = q \le \{m, n\} \tag{1}$$

where $\mathbf{y}$: $n\times1$ vector of observations, $\mathbf{A}$: $n\times m$ design matrix, ξ : $m\times1$ vector of unknowns (parameters), $\mathbf{e}$: $n\times1$ vector of measurement errors, σ_0^2 : variance factor, $\mathbf{P}$: $n\times n$ weight matrix for the observations, and $rk(\cdot)$: rank of matrix.

The normal equation can then be derived by minimizing the quadratic form $\mathbf{e}^{\mathbf{T}}\mathbf{P}\mathbf{e}$, given by:

$$\mathbf{N}\hat{\boldsymbol{\xi}} = \mathbf{c}, \text{ with } [\mathbf{N}, \mathbf{c}] = \mathbf{A}^{\mathbf{T}}\mathbf{P}[\mathbf{A}, \mathbf{y}]. \tag{2}$$

In principle, relative GPS positioning adopts the interferometric technique so that additional constraints are imposed to compute the absolute coordinates of the stations. Various types of constraints may be imposed to avoid the rank deficiency problem. However, some types of constraints cause network distortion, which is not suitable for the deformation analysis. Therefore, the minimum constraint solution also called the "inner constraint solution", which minimizes the norm of the parameter vector, is commonly used as it does not affect the network geometry. The minimum constraint solution can be obtained by imposing the constraint $\mathbf{E}\boldsymbol{\xi} = \mathbf{0}$ (Snow, 2002; Schaffrin, 2003). $\mathbf{E}$ is defined such that its transpose forms a basis for the null space of $\mathbf{A}$, and the minimum constraint solution is then given by:

$$\hat{\boldsymbol{\xi}} = \left(\mathbf{N} + \mathbf{E}^{\mathbf{T}}\mathbf{E}\right)^{-1}\mathbf{c} = \mathbf{N}^{+}\mathbf{c}. \tag{3}$$

where $(\cdot)^{+}$: pseudoinverse, also called the *Moore-Penrose inverse* (Koch, 1999).

The cofactor matrix for unknowns $\mathbf{Q}_{\hat{\xi}}$, the residual vector $\tilde{\mathbf{e}}$, the quadratic form of the weighted sum of residuals Ω, and the estimated variance factor $\hat{\sigma}_0^2$ can be derived by using Eqs. (1) and (3):

$$\mathbf{Q}_{\hat{\xi}} = \mathbf{N}^{+}, \; \tilde{\mathbf{e}} = \mathbf{y} - \mathbf{A}\hat{\boldsymbol{\xi}}, \; \Omega = \tilde{\mathbf{e}}^{\mathbf{T}}\mathbf{P}\tilde{\mathbf{e}}, \; \hat{\sigma}_0^2 = \frac{\Omega}{f}, \quad f = \text{degrees of freedom} \tag{4}$$

In general, the minimum constraint solution shown in Eq. (3) is a datum-dependent solution. This means that the coordinates obtained in the two periods cannot be compared directly because the estimated coordinates are not based on the common datum. To solve this problem, it is necessary to apply a so-called S-transformation to both solutions obtained from two periods (Gründig *et al*., 1985). It should be noted that the geometric shape of the network does not change due to the S-transformation (Koch, 1999). Then, the coordinate vector and its covariance matrix with respect to the new datum can be computed as shown in Eqs. (5) and (6), respectively (Denli, 2004; Acar *et al*., 2008):

$$\hat{\boldsymbol{\xi}}_j = \mathbf{S}\hat{\boldsymbol{\xi}}_i \tag{5}$$

$$\mathbf{Q}_j = \mathbf{S}\mathbf{Q}_i\mathbf{S}^{\mathbf{T}} \tag{6}$$

$$\mathbf{S} = \mathbf{I} - \mathbf{G}(\mathbf{G}^{\mathbf{T}}\mathbf{I}_S\mathbf{G})^{-1}\mathbf{G}^{\mathbf{T}}\mathbf{I}_S \tag{7}$$

where $\mathbf{S}$: S-transformation matrix, $\mathbf{I}$: identity matrix, $\mathbf{I}_S$: datum selection matrix.

For the three-dimensional networks, the matrix $\mathbf{G}$ is as follows:

$$\mathbf{G}^{\mathbf{T}} = \begin{bmatrix} 1 & 0 & 0 & \cdots & 1 & 0 & 0 \\ 0 & 1 & 0 & \cdots & 0 & 1 & 0 \\ 0 & 0 & 1 & \cdots & 0 & 0 & 1 \\ 0 & -\bar{z}_{10} & \bar{y}_{10} & \cdots & 0 & -\bar{z}_{0} & \bar{y}_{m0} \\ \bar{z}_{10} & 0 & -\bar{x}_{10} & \cdots & \bar{z}_{m0} & 0 & -\bar{x}_{m0} \\ -\bar{y}_{10} & \bar{x}_{10} & 0 & \cdots & -\bar{y}_{m0} & \bar{x}_{m0} & 0 \\ \bar{x}_{10} & \bar{y}_{10} & \bar{z}_{10} & \cdots & \bar{x}_{m0} & \bar{y}_{m0} & \bar{z}_{m0} \end{bmatrix} \tag{8}$$

where $\bar{x}_{i0}$, $\bar{y}_{i0}$, $\bar{z}_{i0}$ (i=1,m): coordinates with respect to the geometric weight center of the network.

In conventional 3D geodetic networks, the number of datum defects is 7 (i.e., 3 translations, 3 rotations, 1 scale factor). However, in the GPS network the number of datum defects is 3, for the number of translations on the three axis directions (Welsch, 1993). To investigate the deformation, testing of the null hypotheses can be introduced as follows (Denli, 2004; Küreç and Konak, 2014):

$$H_0 : \hat{\boldsymbol{\xi}}_{II}^{j} = \hat{\boldsymbol{\xi}}_{I}^{j} \tag{9}$$

The displacement vector and its covariance matrix can be compute and given by

$$\mathbf{d} = \hat{\boldsymbol{\xi}}_{II}^{j} - \hat{\boldsymbol{\xi}}_{I}^{j}, \quad \mathbf{Q}_{\mathbf{d}} = \mathbf{Q}_{\hat{\xi}_I} + \mathbf{Q}_{\hat{\xi}_{II}} \tag{10}$$

$$R = \mathbf{d}^{\mathbf{T}} \left(\mathbf{Q}_{\mathbf{d}}\right)^{+} \mathbf{d} \tag{11}$$

where $\mathbf{d}$: difference vector, $\left(\mathbf{Q}_{\mathbf{d}}\right)^{+}$: cofactor matrix for $\mathbf{d}$.

The combined variance factor $\hat{\sigma}_{0,c}^{2}$ can be computed as follows:

$$\hat{\sigma}_{0,c}^{2} = \frac{f_I \hat{\sigma}_{0,I}^{2} + f_{II} \hat{\sigma}_{0,II}^{2}}{f_c}, \quad f_c = f_I + f_{II} \tag{12}$$

The corresponding test statistic is then computed by:

$$T = \frac{R}{\hat{\sigma}_{0,c}^{2}\, f_{\mathbf{d}}} \tag{13}$$

where $f_{\mathbf{d}}$: rank of $\mathbf{Q}_{\mathbf{d}}$.

If the test value T is greater than the critical value, i.e., $T > F_{1-\alpha, f_{\mathbf{d}}, f_c}$, then we can say that a significant deformation is occurred. Fig. 1 shows the overall procedures applied to investigate the deformation due to the Kyungju earthquake on 12 September 2016.

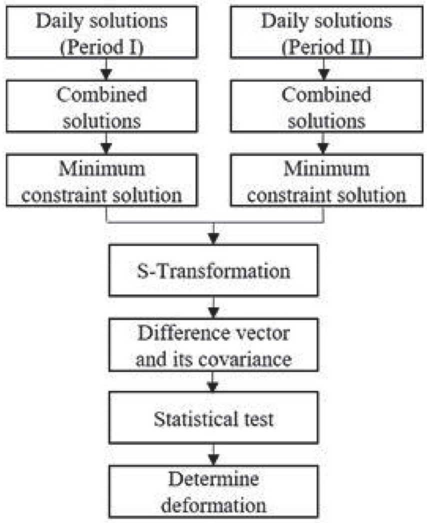

Fig. 1. Flowchart of the deformation analysis

3. Numerical Results

To investigate earthquake-related crustal deformation, a subset of the Korean CORS located within ~100 km from

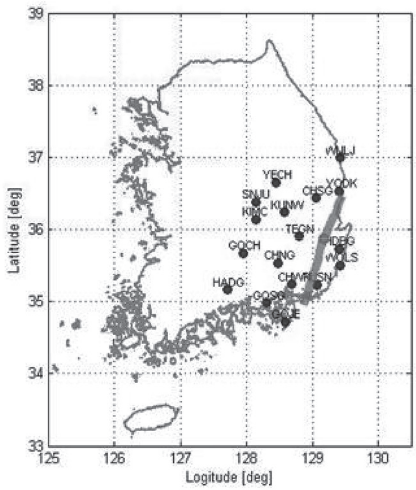

Fig. 2. Location map of Korean CORS and Yangsan geological fault line

Kyungju city, is selected. The total number of selected stations is 17 for the deformation analysis and the locations of the Korean CORS are shown in Fig. 2. The blue and red dots indicate the locations of Korean CORS and Kyungju city, respectively. Also, the Yangsan geological fault line is shown in purple.

The GPS data was collected from the stations shown in Fig. 2 over a 3-month period. The 3-month period is divided into two periods (period I and II) to analyze the deformation between the periods, i.e., two months before and one month after the earthquake, as indicated in Fig. 3.

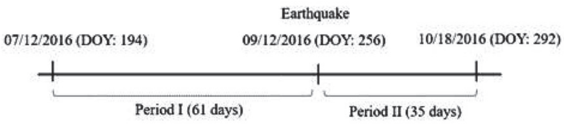

Fig. 3. Data span used for the deformation analysis

The collected data is processed on a daily basis in double difference mode using the *Bernese GPS software package, version 5.2* (Dach *et al*., 2015). Hence, the daily network-based solutions for each day are obtained for both period I and II. It should be noted that the daily solutions are computed by applying tight stochastic constraints on the coordinates of the CHSG station. The parameters in this step include the coordinates of the stations, the total zenith tropospheric delay, and ambiguities.

The combined solutions for each period are computed by accumulating the normal matrix from the daily solutions. The minimum constraint solutions, which are associated with the 3 dimensional Helmert transformation, are obtained for periods I and II, respectively, to avoid network distortion. Table 1 shows the minimum constraint solutions for both periods I and II.

The mean values of the coordinate differences for the X, Y, and Z components are -0.028m, 0.033m, 0.030m, respectively. These coordinates differences may be caused by the fact that each solution for period I and II is computed on different datum. Therefore, the S-transformation using Eq. (5) needs to be applied to each solution to make both solutions refer to the same datum. It should be noted that last row of $\mathbf{G}^T$, which correspond to the scale factor, is not used to detect

Table 1. Minimum constraint solutions (unit: meter)

	Period I			Period II		
Station Name	X	Y	Z	X	Y	Z
CHNG	-3233224.374	4067916.448	3686212.184	-3233224.343	4067916.411	3686212.151
CHSG	-3237145.847	3989513.776	3767338.630	-3237145.816	3989513.743	3767338.599
CHWN	-3260411.353	4070678.491	3659345.351	-3260411.323	4070678.457	3659345.321
GOCH	-3189851.575	4091157.939	3698444.845	-3189851.541	4091157.899	3698444.807
GOJE	-3273540.891	4102034.416	3612576.600	-3273540.862	4102034.383	3612576.571
GOSG	-3243049.309	4105277.505	3636138.736	-3243049.280	4105277.474	3636138.708
HADG	-3192918.472	4129777.905	3652656.572	-3192918.449	4129777.877	3652656.547
HDBG	-3290018.348	4005491.245	3704357.943	-3290018.320	4005491.214	3704357.913
KIMC	-3185110.003	4055952.084	3740570.884	-3185109.978	4055952.050	3740570.850
KUNW	-3211712.202	4026954.380	3749223.408	-3211712.174	4026954.349	3749223.378
PUSN	-3287592.249	4049012.153	3659188.031	-3287592.220	4049012.124	3659188.009
SNJU	-3175473.144	4043362.987	3762213.654	-3175473.118	4043362.956	3762213.627
TEGN	-3241051.626	4030771.806	3719838.557	-3241051.597	4030771.773	3719838.527
WOLS	-3300601.093	4015928.397	3683580.259	-3300601.066	4015928.360	3683580.228
WULJ	-3238396.239	3940665.446	3816730.650	-3238396.211	3940665.414	3816730.621
YECH	-3185564.156	4012511.085	3786513.690	-3185564.131	4012511.055	3786513.664
YODK	-3257453.430	3964411.726	3775960.846	-3257453.401	3964411.693	3775960.816

the possible expansion of the network. Also, corresponding covariance matrices can be computed using Eq. (6) by the error propagation law. The difference coordinate vector and its covariance matrix can be computed using Eq. (10). Table 2 present the coordinate difference vector for each coordinate component.

Table 2. Differences of coordinate after S-transformation (unit: meter)

Station Name	d_x	d_y	d_z
CHNG	-0.0031	0.0041	0.0025
CHSG	-0.0022	0.0003	0.0012
CHWN	-0.0016	0.0017	0.0008
GOCH	-0.0057	0.0078	0.0087
GOJE	-0.0010	-0.0002	-0.0007
GOSG	-0.0001	-0.0011	-0.0014
HADG	0.0048	-0.0049	-0.0052
HDBG	-0.0003	-0.0018	-0.0002
KIMC	0.0027	0.0010	0.0041
KUNW	-0.0008	-0.0019	0.0007
PUSN	-0.0009	-0.0043	-0.0072
SNJU	0.0022	-0.0020	-0.0020
TEGN	-0.0002	0.0005	-0.0002
WOLS	0.0017	0.0035	0.0017
WULJ	0.0003	-0.0003	-0.0003
YECH	0.0035	-0.0024	-0.0033
YODK	-0.0009	-0.0000	0.0006

As shown in Table 2, the magnitudes of the differences after the S-transformation are relatively small when they are compared with those values in Table 1. The estimated variance factor for period I is 3.409 and for period II is 3.031. The degrees of freedom, f_I and f_{II}, are 19820561 and 11850547, respectively. Hence, the combined variance factor $\hat{\sigma}^2_{0,c}$ computed using Eq. (12) is 3.268 and the test statistic T=0.001 is subsequently obtained. For a given confidence level of $\alpha = 5\%$ and $f_{\mathbf{d}} = 45$, it follows that the critical value from the statistical tables $F_{1-\alpha, f_{\mathbf{d}}, f_c}$ is 1.370. The results showed that the test statistic is smaller than the critical value, which indicates that there is no significant deformation between the two periods.

4. Summary and Conclusion

Three months of GPS data was collected and used to investigate the deformation due to the Kyungju earthquake that occurred on 12 September 2016. To investigate the deformation, the coordinates of 17 Korean CORS are computed and analyzed for periods I and II. The minimum constraint approach is selected to avoid network distortion and the S-transformation is applied to the coordinates for each period. Following this, the difference of coordinate vector and its covariance matrix are obtained to compute the test statistic. It is shown that the computed test static quantity is smaller than the critical value when a confidence level of $\alpha = 5\%$ is selected. The results show that no significant deformation is observed due to the Kyungju earthquake. Therefore, it can be said that the re-measurement or re-establishment of geodetic control points is not necessary.

Acknowledgment

This work was funded by the Korean Meteorological Administration Research and Development Program under Grant KMIPA2015-3071. The author would like to thank Prof. Tae-Suk Bae at the Sejong University and Dr. Il-Young Che at the Korean Institute of Geoscience and Mineral Resources for their valuable comments on this research.

References

Acar, M., Ozludemir, M.T., Erol, S., Celik, R.N., and Ayan, T. (2008), Kinematic landslide monitoring with Kalman filtering, *Nat. Hazards Earth Syst. Sci.*, Copernicus Publications on behalf of the European Geosciences Union, Vol. 8, No. 2, pp. 213-321.

Ananga, N. (1991), Least-Squares adjustments of seasonal levelling, *J. Surv. Eng.*, Vol. 117, No. 2, pp. 67-76.

Barda, W. (1973), *S-transformation and criterion matrices*, Netherlands Geodetic Commission Publications on Geodesy, New Series, Delft, Vol. 5, No. 1, 168p.

Dach, R., Lutz, S., Walser, P., and Fridez, P. (2015), *Bernese GNSS Software Version 5.2 Manual*, Astronomical

Institute, University of Bern.

Denli, H.H. (2004), Crustal deformation analysis in the Marmara Sea Region, *J. Surv. Eng.*, Vol. 130, No. 4, pp. 151-155.

Erdoğan, S., Şahin, M., Tiryakioğlu, İ., Gülal, E., and Telli, A.K. (2009), GPS velocity and strain rate fields in southwest Antolia from repeated GPS measurements, *Sensors*, Vol. 9, pp. 2017-2034.

Even-Tzur, G. (2011), Deformation analysis by means of extended free network adjustment constraints, *J. Surv. Eng.*, Vol. 137, No. 2, pp. 47-52.

Gründig, L., Neureither, M., and Bahndorf, J. (1985), Detection and localization of geometric movements, *J. Surv. Eng.*, Vol. 111, No. 2, pp. 118-132.

Hager, B.H., King, R.W., and Murray, M.H. (1991), Measurements of crustal deformation using the Global Positioning System, *Annu. Rev. Earth Planet*, Vol. 19, pp. 351-382.

Hamdy, A.M., Park, P.-H., and Lim, H.-C. (2005), Horizontal deformation in South Korea from permanent GPS network data, 2000-2003, *Earth Planets Space*, Vol. 57, pp. 77-82.

Koch, K.R. (1999), *Parameter Estimation and Hypothesis Testing in Linear Models*, Berlin Heidelberg, New York, Springer-Verlag, 333p.

Küreç, P. and Konak, H. (2014), A priori sensitivity analysis for densification GPS networks and their capacities of crustal deformation monitoring: a real GPS network application, *Nat. Hazards Earth Syst. Sci.*, Vo. 14, pp. 1299-1308.

Lin, K.-C., Hu, J.-C., Ching, J.-C., Angelier, J., Rau, R.-J., Yu, S.-B., Tsai, C.-H., Shin, T.-C., and Huang, M.-H. (2010), GPS Crustal deformation, strain rate, and seismic activity after the 1999 Chi-Chi earthquake in Taiwan, *J. Geophy. Res.*, Vol. 115, B07404, doi:10.1029/2009JB006417.

Liu, R., Li, J., Fok, H.S., Shum, C.K., and Li, Z. (2014), Earth surface deformation in the North China plate detected by joint analysis of GRACE and GPS data, *Sensors*, Vol. 14, pp. 19861-19876.

Miura, S., Sato, T., Tachibana, K., Satake, Y., and Hasegawa, A. (2002), Strain accumulation in and around Ou Backbone Range, northeastern Japan as observed by a dense GPS network, *Earth Planets Space*, Vol. 54, pp. 1071-1076.

Papo, H. and Stelzer, D. (1985), Relative error analysis of geodetic networks, *J. Surv. Eng.*, Vol. 111, No. 2, pp. 133-139.

Schaffrin, B. (2003), *Advanced Adjustment Computations, Lecture Notes (GS762)*, Dept. of Geodetic Science, Ohio State University, Columbus, Ohio, USA.

Snow, K.B. (2002), *Applications of Parameter Estimation and Hypothesis Testing to GPS Network Adjustments*, Report No. 465, Dept. of Geodetic Science, The Ohio State University, Columbus, Ohio, USA.

Welsch, W.M. (1993), A general 7-parameter transformation for the combination, comparison and accuracy control of terrestrial and satellite network observations, *Manuscr. Geod.*, Vol. 18, pp. 295-305.